Design of a Hybrid Common - Mode EMI Filter for Traction Inverters in Electrical Vehicles

Denis Müller[1], Konstantin Spanos[2], Michael Beltle[1], Stefan Tenbohlen[1]

[1] University of Stuttgart, Germany
[2] Robert Bosch GmbH, Germany

Corresponding author: Denis Müller, denis.mueller@ieh.uni-stuttgart.de

The Power Point Presentation will be available after the conference.

Abstract

Higher power density due to silicon carbide switches, rising battery voltages up to 800 V and the mechanical benefits of unshielded battery cables require bigger EMI filters necessary for traction inverters in electrical vehicles. In order to counteract this trend, hybrid EMI filters, which are a combination of passive and active components, represent a promising opportunity to reduce the size of inductive filter elements. This paper presents a design approach and a first prototype of a hybrid filter for an automotive traction inverter. Different filter topologies are discussed in order to find the best match for the use case. Finally, the prototype's attenuation is evaluated in a CISPR 25 standard test setup.

1 Introduction

Due to high voltage gradients during the switching operation and battery voltages up to 800 V, the traction inverter of the electrical drive is the dominant source for electromagnetic interference (EMI) in an electric vehicle. Therefore, additional EMI filters are unavoidable. However, installation space has always been precious and traction inverter's EMI filters are bulky due to the need of low frequency attenuation.

In recent years, several publications determine the benefit of EMI filter optimization using algorithms to reduce the installation space [1], [2], [3]. Nevertheless, the size of the most space-consuming element, the common mode choke (CMC), is difficult to reduce, because the winding of the CMC has to carry the whole operational current.

Several studies have shown, that the greatest attenuation of active EMI filters is achieved in the lower frequency range between 150 kHz and a few MHz [4]-[13]. This is the same spectrum where CMCs are required to get significant noise attenuation. This offers the possibility to combine both, the passive and active EMI filter, to create a smaller hybrid filter compared to only passive filters instead of building up high frequency analog circuits, required for an only active EMI filter [6], [13]. For this purpose [4] presents an active filter to reduce the required CMC. The principal of different active and hybrid EMI filters is demonstrated in [4]-[13]. Nevertheless, most of these filters are operating at small signal amplitudes, where Operational Amplifiers (Op-Amps) output specifications meet the required compensation signals. In traction inverters, the required compensation signals are usually larger than the output specifications of a single Op-Amp.

This paper addresses this issue and presents a high-level design proposal for a hybrid common-mode EMI filter for traction inverters in electrical vehicles. Section 2 describes the design process for the active and passive filter stages, which can be combined to enlarge the frequency range. The hybrid filter is evaluated in a laboratory test setup according to CISPR25, presented in Section 3. The conclusion is given in Section 4.

2 Design of the Hybrid Filter

The design of the hybrid filter can be divided into two parts. The first part is the design of the active stage. In the second part, the passive filter stage can be designed accordingly. The passive filter design contains the choice of the passive topology, which is given by the dynamic range of the active circuit. The hybrid filter is designed to suppress common mode (CM) emissions.

Following this scheme, the next sections will explain the development process for the entire proposed hybrid filter.

2.1 Design of the active filter stage

Active EMI filters are separated in two categories, due to their control loop in feedforward and feedback types [13]. Feedforward type filters need a unity gain to suppress the disturbance ideally and have in each configuration a stable transfer function. Feedback type filters need an infinite gain due to their configuration as a control loop. This leads to a transfer function, in which stability problems can occur. In our case, the feedback type has been chosen, because the unity gain of feedforward topology is difficult to implement in practice. There are tolerances in assembly parts, which leads a higher gain than unity. Therefor, the filter attenuation cannot be guaranteed anymore.

In general, an active filter consists of a sensing stage, an inverting amplifier and an injection stage. Figure 1 shows the block diagram of an active feedback filter. Basically, it is a control loop, which cancels the disturbance on the DC supply of the traction inverter. Sensing and injection elements can be capacitors or transformers. By combining the different sensing and injection methods, there are four different topologies which can be implemented. To select the suited topology, it is necessary to rate the expected insertion loss of the different combinations.

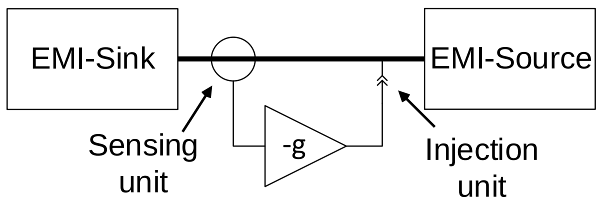

Fig. 1: Block diagram of an active feedback EMI filter

By using a capacitor, it is possible to sense a voltage or inject a current. Using a transformer, current sensing and voltage injection can be realized. The use of a transformer as sensing or injection element is difficult. The DC current in the electrical drive can be up to 400 A. Due to high currents it is not possible to realize the necessary turns ration on primary or secondary side. On the one hand, it is difficult to realize more than one turn mechanically, due to high cross sections of the conductors. On the other hand, there may be saturation of the magnetic core.

Therefore, the realization of the proposed active EMI filter is based on capacitors for both, sensing and injection parts. This allows a filter that is decoupled from the operating currents of the HV lines. The single phase equivalent circuit is shown in Fig. 2. For the proposed system, each phase contains one separate active filter stage. For simplification, the passive filter stage is not shown

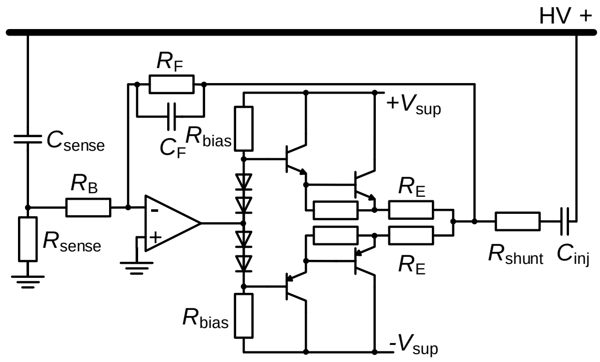

Fig.2: Equivalent single phase circuit of the active feedback filter stage

in this circuit.

The sensing stage is designed as a high pass filter with the cut off frequency

$$f_g = \frac{1}{2\pi \cdot R_{sense} \cdot C_{sense}} = 18\ \mathrm{kHz} \qquad (1)$$

The compensation signal is injected through three parallel 47 nF capacitors, in the equivalent circuit simplified to C_{inj}. By using parallel capacitors, their combined series inductance can be reduced to enlarge the bandwidth of the injection circuit. For measuring the injected current during operation, a shunt resistor R_{Shunt} is placed in the injection circuit.

The two stage amplifier is built using an Op-Amp as pre-amplifier stage and a complementary push-pull amplifier as power amplifier stage. The push-pull amplifier is built up with two complementary Darlington transistor pairs, assembled of discrete power bipolar junction transistors (BJT) [15]. The Darlington pairs are biased via a bias resistor R_{bias} and two diode voltage drops. The amplifiers feedback is realized by R_B and R_F, paralleled with a capacitor C_F to split up the poles of the closed control loop. The feedback loop increases the stability of the amplifier.

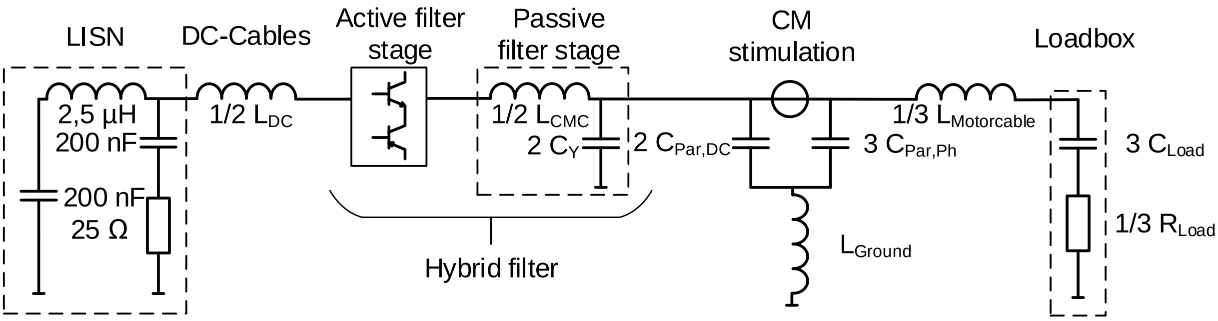

Fig. 3: Single phase CM equivalent circuit of the test setup with active and passive filter stage

2.2 Design of the passive filter stage

After the design of the active filter stage, the passive filter stage can be configured accordingly. The passive stage contains of a C_Y capacitor pair in combination with a common mode choke (CMC). Both elements are required to reduce the disturbances to such a level that the active part will not get into overload. Due to high attenuations of the active filter part in low frequency range, the main attenuation of the passive filter is required above several MHz.

Figure 3 shows the single phase equivalent circuit of the test setup according to [5] with included hybrid filter. The size of the Y-capacitors is 220 nF and a single turn CMC with a nanocrystalline core material with a permeability of 30,000 is used. The size of the components was chosen to decrease the disturbance at the input terminals of the active stage in a way that operation with a bipolar supply voltage of 12 V is possible. A concrete EMC limit was not considered for implementation of the filter.

3 Evaluation of the hybrid CM filter

The hybrid system is build and tested in a setup according to CISPR 25 component test. Figure 4 shows a picture of the test setup of the inverter in an anechoic line shielded enclosure (ALSE). Unshielded cables are used for DC-supply. The system is tested at a DC-voltage of 300 V. With a duty-cycle of 50 %, the filter is tested at worst case CM disturbance. A loadbox with an inductance of 3x 160 µH and three discrete phase to ground capacitors with C_G = 2.2 nF is used.

In the following measurements, the conducted emissions at the LISN are measured with an EMI receiver. Therefore, a 0° power combiner is used to separate the CM component of disturbance voltage. The block diagram and a picture of the measurement is shown in Fig. 4.

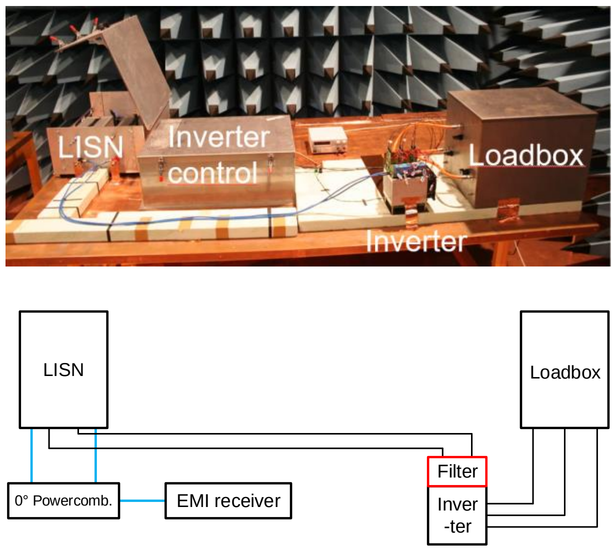

Fig. 4: Test setup according to CISPR25

The comparison between only passive and hybrid operation mode of the filter and the raw emissions of the inverter is depicted in Fig. 5. The measurement shows the CM part of the disturbance voltage at the LISN. The blue curve represents the measurement in only passive operation, the red curve in hybrid operation and the yellow curve the raw emissions. In the frequency range from 150 kHz up to 1 MHz the active part of the filter provides an additional reduction of about 10 – 25 dB, compared to the passive part. Below 500 kHz, the attenuation of the passive filter stage is only 15 – 20 dB. With up to 25 dB, the active filter part provides a significant increase in attenuation. In this frequency range, the active filter part compensates the passive filters disadvantages. Up to 3 MHz the hybrid filter achieves an additional attenuation from 8 – 3 dB. Due to the high frequency behavior of the BJTs, the spectrum is raised around 4 dB in frequencies over 3 MHz.

There, the phase shift of disturbance and compensation signal differs from 180 ° and the disturbance is increased. The bandwidth of the hybrid filter could be enlarged by using transistors for the Darlington configuration with a high transit frequency f_T, fast switching times and medium current capability [15]. Due to the achieved attenuation, the active filter stage can be used to support the passive filter in low frequency range. This can provide savings in inductive filter components and save installation space of EMI filter consequentially.

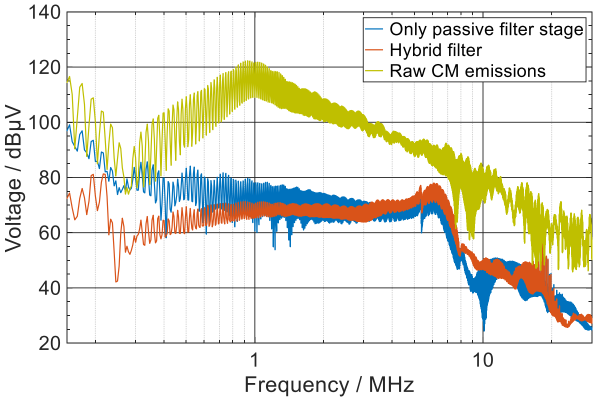

Fig. 5: Measurement of conducted CM emissions at LISN

Besides relevant frequency bands specified in CISPR 25, the combination of a hybrid filter also achieves higher attenuation in frequency range below 150 kHz. Figure 6 compares the conducted CM emissions of the only passive filter stage and the hybrid filter in the frequency range from 9 kHz to 150 kHz.

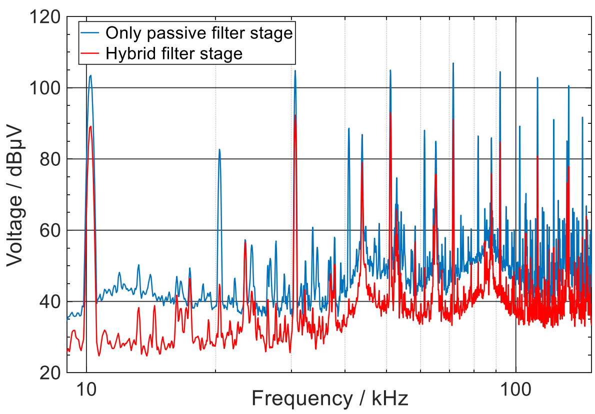

Fig. 6: Measurement of conducted CM emissions at LISN for frequencies below 150 kHz

For the odd harmonics of the inverters switching frequency f_C of 10.1 kHz, the highest attenuation of 25 dB can be measured at 131.3 kHz. Attenuation decreases towards lower frequencies due to the lower corner frequency of the active filters sensing high pass. Nevertheless, at the fundamental switching frequency f_c of 10.1 kHz a attenuation of 15 dB can be achieved. For even harmonics a nearly complete cancellation can be observed. The underlying mechanism is not completely known yet and will be in focus of future investigations.

4 Conclusion

The combination of a passive filter with an active compensation part provides an enhancement of filter attenuation in the lower frequency range. With a common passive filter, it is difficult to improve filtering performance in this frequency range because bulky inductors are required.

The paper presented a way to design a hybrid EMI filter. By using a push-pull amplifier, it was possible to build up a prototype filter for a 300 V application. Measurements pointed out the increase of filter attenuation in lower frequency range caused by the active filter stage. The higher attenuation also can be found in measurements below the standardized frequency range. If attenuation in this frequency range is required, large common mode chokes are necessary. According to this benefit, the presented combination provides more flexibility for the EMI suppression in the electrical drive of vehicles. The economic advantage could be given under harsher EMC requirements, like the use of unshielded DC cables or more strict EMC standards below 150 kHz.

5 References:

[1] J.L.Schanen, A. Baraston, M. Delhommais and P. Zanchetta, “Sizing of Power Electronics EMC Filter Using Design by Optimization Methodology”, 7th Power Electronics, Drive Systems & Technologies Conference (PEDSTC’16), Iran University of Science and Technology, Teheran, Iran, 2016, pp. 279-284

[2] G. Ala, G.C. Giaconia, G. Giglia, M.C. Di Piazza, M. Luna, G. Vitale and P. Zanchetta, Computer Aided Optimal Design of High Power Density EMI Filters”, IEEE 16th International Conference on Environmental and Electical Engineering (EEEIC’16), Florence, Italy,2016

[3] D. Mueller, M. Beltle, S. Tenbohlen, “Automated Filter Optimization for High-Voltage Cable Harness based on Circuit Simulations for Conducted Emissions Prediction“, International Symposium on Electromagnetic Compatibility (EMC Europe 2018), Amsterdam, The Netherlands, 2018

[4] W. Chen, X. Yang and Z. Wang, “An Active EMI Filtering Technique for Improving Passive Filter Low-Frequency Performance” IEEE Transactions on Electromagnetic Compatibility, Vol.48, No.1, February 2006

[5] A. Amaducci, “Design of a Wide Bandwidth Active Filter for Common Mode EMI suppression in Automotive systems”, IEEE International Symposium on Electromagnetic Compatibility & Signal/Power Integrity (EMCSI), Washington, DC, USA, 2017, pp. 612-618

[6] S. Wang, Y.Y. Maillet, F. Wang, D. Boroyevich and R. Burgos, “Investigation of Hybrid EMI Filters for Common-Mode EMI Suppression in a Motor Drive System”, Trans. on Power Electronics, Vol. 25, No. 4, April 2010, pp. 1034-1045

[7] M.C. Di Piazza, G. Tinè and G. Vitale, “An Improved Active Common-Mode Voltage Compensation Device for Induction Motor Drives”, IEEE Trans. on Industrial Electronics, Vol. 55, No. 4, April 2008, pp.1823-1834

[8] R. Goswami, S. Wang and Y. Zhang, “Modeling, Analysis and Design of Differential Mode Active EMI Filters with Feedforward and Feedback Configurations for AC-DC Converters”, IEEE Energy Conversion Congress and Exposition (ECCE), Milwaukee, WI, USA, 2016

[9] S. Mollov and L. Rambaud, “A Fully-Isolated Robust Common-Mode Hybrid Filter”, International Conference on Integrated Power Electronic Systems (CIPS),Stuttgart, Germany, 2018

[10] P. Pairodamonchai, S. Suwankawin and S. Sangwongwanich, “Design and Implementation of a Hybrid Output EMI Filter for High-Frequency Common-Mode Voltage Compensation in PWM Inverters”, IEEE Trans. on Industrial Applications, Vol. 45, No. 5, September/October 2009, pp.1647-1659

[11] D. Shin, J. Kim, C. Son, S. Jeon. B. Cho and J. Han, “A Simple Low-Cost Common Mode Active EMI Filter Using a push-pull Amplifier”, IEEE Energy Conversion Congress and Exposition (ECCE), Milwaukee, WI, USA, 2016

[12] D. Shin, S. Kim, G. Jeong, J. Park, K.J. Han and J. Kim, “Analysis and Design Guide of Active EMI Filter in a Compact Package for Reduction of Common-Mode Conducted Emissions” IEEE Trans. on Electromagnetic Compatibility, Vol. 57, No. 4, August 2015, pp. 660-671

[13] W. Chen, X. Yang and Z. Wang, “Systematic evaluation of hybrid active EMI filter based on equivalent circuit model”, Power Electronics Specialists Conference (PESC), Jeju, South Korea, 2006, pp. 2711-2717

[14] P. Hillenbrand, C. Keller, K. Spanos and S. Tenbohlen, “Understanding Conducted Emissions from an Automotive Inverter Using a Common-Mode Model”, IEEE and EMC Joint Conference, Dresden, Germany, 2015, pp. 685-690

[15] P. Horowitz and W. Hill, “The Art of Electronics”3rd Ed., Cambridge University Press, 2015, ISBN 978-0-521-80926-9